

Interference effects in isolated Josephson junction arrays with geometric symmetries

Dmitri A. Ivanov^a, Lev B. Iosevich^b, Vadim B. Geshkenbein^a, and Gianni Blatter^a

^a Theoretische Physik, ETH-Honggerberg, CH-8093 Zurich, Switzerland

^b Center for Materials Theory, Physics Department, Rutgers University, Piscataway, NJ 08854 USA
(February 9, 2001)

As the size of a Josephson junction is reduced, charging effects become important and the superconducting phase across the link turns into a periodic quantum variable. Isolated Josephson junction arrays are described in terms of such periodic quantum variables and thus exhibit pronounced quantum interference effects arising from paths with different winding numbers (Aharonov-Casher effects). These interference effects have strong implications for the excitation spectrum of the array which are relevant in applications of superconducting junction arrays for quantum computing. The interference effects are most pronounced in arrays composed of identical junctions and possessing geometric symmetries; they may be controlled by either external gate potentials or by adding/removing charge to/from the array. Here we consider a loop of N identical junctions encircling one half superconducting quantum of magnetic flux. In this system, the ground state is found to be non-degenerate if the total number of Cooper pairs on the array is divisible by N , and doubly degenerate otherwise (after the stray charges are compensated by the gate voltages).

I. INTRODUCTION

Josephson junction arrays are excellent tools for exploring quantum-mechanical behavior in a wide range of parameter space¹. The charge and phase on each island provide a set of conjugate quantum variables, allowing for dual descriptions of the array either in terms of charges (Cooper pairs) hopping between the islands or in terms of vortices hopping between the plaquettes of the array². This opens the door for the set up and manipulation of interesting quantum interference effects in Josephson junction arrays: in a magnetic field, charges pick up additional Aharonov-Bohm phases and hence the properties of the array depend on the field strength. In the dual language, vortices moving around islands gain phases proportional to the average charges on the islands (Aharonov-Casher phases)^{3;4}. These features have recently been used in various proposals for solid state implementations of qubits for quantum computing, based on either the charge⁵ or phase^{6;8} degree of freedom in Josephson junction arrays.

In this paper we study an interference effect in electrically isolated Josephson junction arrays which renders the ground state and excitation spectrum sensitive to the total charge on the array. This effect combines the dual descriptions in terms of charge or phase: i) in the limit where the charging energy E_C is much larger than the Josephson energy E_J , the fluctuations of charge on the islands are small and the system is equivalent to strongly repulsive bosons (Cooper pairs) hopping between islands; the total charge then determines the number of such bosons and hence the structure of the spectrum. ii) In the opposite limit of large Josephson energy E_J , the phase fluctuations are small and the spectrum is determined by phase tunneling between classical minima of the Josephson energy; the total charge on the array then determines the interference between different tunneling trajectories

via the Aharonov-Casher effect. These interference effects, where the ground state and the excitations may change degeneracies depending on the total charge on the array, are most pronounced in small arrays with geometric symmetries; for the symmetric loops considered in this paper they coincide in the charge- and phase-dominated limits and persist at arbitrary ratio of the Josephson- to charging energy. In mathematical terms, the total charge on the array enters its symmetry group producing a central extension⁹. The irreducible representations are then classified by the total charge, and their dimensions (and associated level degeneracies) depend on the charge on the array.

In experimental realizations of Josephson junction arrays, the charges and potentials on the islands are affected by a number of external factors such as differences

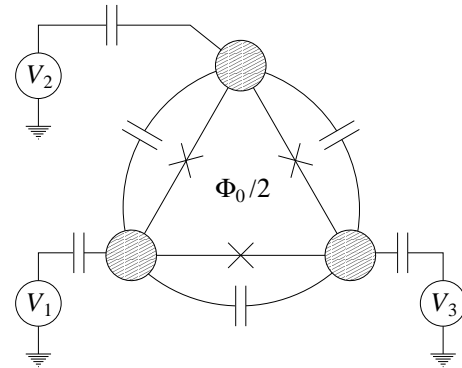


FIG. 1. A superconducting phase qubit consists of a small inductance loop made from N superconducting islands connected by Josephson junctions and capacitively coupled to each other and to the ground (the case $N = 3$ is shown here). The loop is placed in an external magnetic field producing one half superconducting flux quantum through the loop.

in island size, background charges, charges localized at impurities, etc. All these factors produce random charge offsets on the islands which distort the quantum interference pattern (see e.g. the discussion of offset charges in Ref. 1). In order to observe the quantum interference effects predicted in this paper the potentials of the islands should be adjustable via external capacitive gates. The offset charges should then be compensated by appropriate tuning of the gate voltages; such a procedure was successfully carried out in a transport measurement involving two islands¹⁰ and should also be possible for the system considered in this paper. We also assume the absence of quasiparticles on the islands. Firstly, this requires the temperature to be sufficiently low to eliminate thermal quasiparticles. Secondly, the total number of electrons on the array must be even in order to exclude unpaired charge due to the parity effect.

In the following we study the simplest setup exhibiting these interference effects, a closed low-inductance loop with $N \geq 3$ identical Josephson junctions and pierced by one-half superconducting flux quantum (Fig. 1). Such loops have been proposed as possible realizations for superconducting phase quantum bits^{6,8} and a successful quantum superposition of the two qubit states has been reported recently¹¹. While in the original qubit design the loop has been made asymmetric in order to suppress the interference of different tunneling paths^{6,8}, it is this interference that we study in the present paper where we assume the islands and contacts to be nearly identical (the required precision will be specified at the end of the paper). The ground state degeneracy of such a symmetric Josephson-junction loop is found to depend periodically on the total charge Q with period $2eN$, N is the number of islands in the loop. In particular, in the phase-dominated regime $E_J \gg E_C$ the Josephson energy of the fully frustrated loop exhibits two equivalent minima describing states with currents circulating in opposite directions. Tunneling between these minima produces a splitting between these levels which is determined by the charges q_i (in units of $2e$) induced on the islands,

$$E = E_0 \left[1 + e^{2i q_1} + e^{2i(q_1 + q_2)} + \dots + e^{2i(q_1 + \dots + q_{N-1})} \right]; \quad (1)$$

and which vanishes for $(Q = 2e) \notin 0 \pmod{N}$ (the sum of all induced charges q_i equals Q , and the expression (1) is symmetric under circular permutation of the islands). This result is the consequence of the interference of different tunneling paths connecting the two minima where the relative phases of the tunneling amplitudes depend on the charges q_i (a similar effect was predicted for the S-S-S double junction in Ref. 12). The induced charges q_i may be tuned by either gate voltages (redistributing the existing charge) or by adding/removing extra charge to/from the array. E.g. suppose that all charges q_i have been set to zero by fine tuning the gate voltages, thus

maximizing the splitting. Then adding (or removing) a charge Q at fixed relative potentials adds a value $Q = 2eN$ to each induced charge q_i and closes the gap: the splitting is present when the charge $Q = 2e$ is divisible by N and absent otherwise. A similar result applies for the opposite limit $E_C \gg E_J$ where the ground state is non-degenerate with the next excited state an energy E_C away if $Q = 2e$ is divisible by N ('insulating' state), while it is degenerate with an excitation gap of order E_J if $Q = 2e \notin 0 \pmod{N}$ ('metallic' state). Indeed, this Q -dependence of the ground state degeneracy will be explained using symmetry considerations valid in the entire range of couplings $E_J = E_C$.

The paper is organized as follows. In Section II, we define the model and prove the periodic dependence of the excitation spectrum on the total charge Q , for a symmetric loop. In Sections III and IV, we treat the limits $E_J \gg E_C$ and $E_J \ll E_C$, respectively. Section V contains the analysis of the symmetries of the loop. Finally, in Section VI we discuss the physical requirements for observing the charge-dependent interference effects.

II. MODEL AND PERIODIC Q -DEPENDENCE OF THE SPECTRUM

The Hamiltonian describing the qubit in Fig. 1 takes the form

$$H = \frac{1}{2} \sum_{ij} Q_i (C^{-1})_{ij} Q_j + \sum_i V_i Q_i + \sum_i U_i (\theta'_{i+1} - \theta'_i - a_{i,i+1}); \quad (2)$$

Here, θ'_i are the phases on the islands, $Q_i = i\partial/\partial\theta'_i$ are the charge operators conjugate to θ'_i (we measure Q in units of $2e$ from now on), $(C^{-1})_{ij}$ is the inverse capacitance matrix, V_i are the gate voltages applied to the islands, U_i are the Josephson energies of the junctions, and $a_{i,i+1}$ is the electromagnetic vector potential induced by the external magnetic field ($i+1$ in the indices should be understood modulo N). This Hamiltonian acts on the wave functions $(\theta'_1; \dots; \theta'_N)$ which are periodic in all their variables,

$$(\theta'_1; \dots; \theta'_{i+2}; \dots; \theta'_N) = (\theta'_1; \dots; \theta'_i; \dots; \theta'_N); \quad (3)$$

In general, the boundary conditions (3) may contain arbitrary phase shifts $e^{i\phi_i}$ incorporating the effect of background charges. They can be manipulated by the gate voltages V_i and we assume them to vanish through appropriate fine tuning¹⁰ (this is equivalent to adjusting the zero positions of the gate voltages). We assume that this tuning is performed once in the beginning of the experiment and later measure the gate voltages relative to these reference values.

Since the potential term in the Hamiltonian (2) contains only phase differences $\phi_i - \phi_j$, it has the symmetry of rotating all the phases by the same angle: $(\phi_1; \dots; \phi_N) \rightarrow (\phi_1 + \phi; \dots; \phi_N + \phi)$. Equivalently, the total charge $Q = \sum_i Q_i$ is conserved (i.e., the charge Q commutes with the Hamiltonian H) and we may project the Hilbert space onto the subspace with a given total charge Q before diagonalization, implying the transformation rule

$$(\phi_1 + \phi; \dots; \phi_N + \phi) = e^{i\phi Q} (\phi_1; \dots; \phi_N) \quad (4)$$

for the simultaneous rotation of all the phases by ϕ . From the periodicity of ϕ , it immediately follows that Q is integer, i.e., the total charge must be a multiple of $2e$ (this is in fact an implicit assumption when writing the Hamiltonian (2) in terms of phases only). In the following we shall discuss the symmetric loop, postponing the effects of asymmetry till the end of the paper. Here, by symmetry we mean $(C^{-1})_{ij} = (C^{-1})_{i+k;j+k}$ for the Coulomb term and equality of all Josephson terms $U_i(\phi)$. This implies that the loop is invariant under circular permutation of the islands. Also, if the flux through the loop is exactly one half flux quantum, the loop is invariant under 'flips' changing the direction of the current.

The excitation spectrum of the symmetric loop periodically depends on the total charge Q with the period N (up to overall shifts): the unitary operator

$$U : \psi \rightarrow e^{i(\phi_1 + \dots + \phi_N)} \psi \quad (5)$$

increases the charge on all the islands by one, $U^{-1} Q_i U = Q_i + 1$, and therefore the sector with total charge Q maps onto the one with total charge $Q + N$. On the other hand,

$$U^{-1} H U = H + \sum_i (C^{-1})_{ij} Q_j + \frac{1}{2} \sum_{ij} (C^{-1})_{ij} + \sum_i V_i; \quad (6)$$

P

If all the islands are equivalent, then the sum $\sum_i (C^{-1})_{ij}$ is independent of j and

$$U^{-1} H U = H + \frac{N}{C} Q + \frac{N}{2} + \sum_i V_i; \quad (6)$$

where $C = N \sum_i (C^{-1})_{ij}^{-1} = \sum_{ij} C_{ij}$ is the total capacitance of the loop. Thus the operator U maps the eigenfunctions of the Hamiltonian in the sector with charge $Q + N$ shifting them in energy by a constant as given by (6), thus proving our statement about the periodic Q -dependence of the excitation spectrum.

III. LEVEL SPLITTING IN THE $E_J \gg E_C$ LIMIT

In the phase-dominated regime with $E_J \gg E_C$ the low-energy states of the Josephson junction loop are determined by the classical minima of the Josephson energy as corrected by weak quantum tunneling (due to

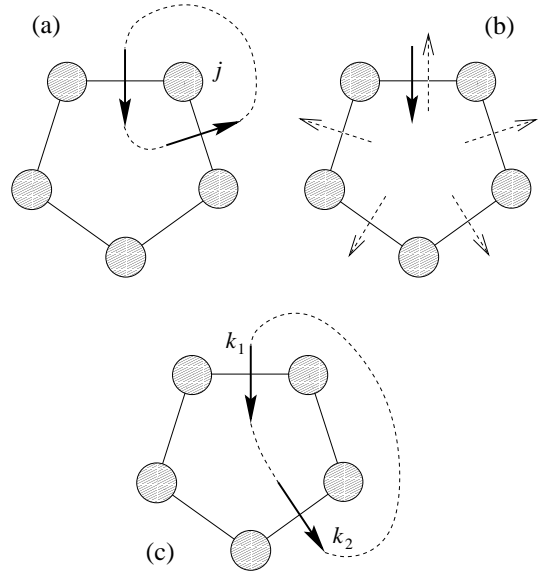


FIG. 2. (a) One flux quantum moving around the j -th island; (b) One of the N possible tunneling trajectories: one flux quantum enters the loop through one of the junctions and leaves divided uniformly between all junctions; (c) The phase difference between two tunneling trajectories with flux entry through the junctions k_1 and k_2 is given by the Aharonov-Bohm phase arising from one flux unit circling the (charged) islands in between. Note that closing the flux trajectory in (c) on the opposite side produces the same phase because Q is an integer.

the finite charging energy). Here, we consider a symmetric loop pierced by half a quantum of magnetic flux, $a_{i,i+1} = \frac{1}{2}$, and we choose to work in a gauge with $a_{i,i+1} = \frac{1}{2} - N$ for all i . In the limit $E_J \gg E_C$ the only constraint on the potential $U_i(\phi)$ is the double degeneracy of the total Josephson energy as a function of the phases ϕ_i (e.g., this requirement is satisfied for tunneling junctions with $U_i(\phi) = E_J \cos \phi$ and $N \equiv 3$). The two potential minima are determined by the phase configurations $\phi_i = 0$ and $\phi_i = (2 - N)\phi_i$ (and all configurations obtained from these two by the continuous symmetry $\phi_i \rightarrow \phi_i + \phi$). These two minima involve different directions of the Josephson current, circulating the loop clockwise or counter-clockwise. The continuous symmetry $\phi_i \rightarrow \phi_i + \phi$, $i = 1; \dots; N$ implies the quantization of the total charge Q as discussed above.

In the following it will be convenient to incorporate the voltage terms $V_i Q_i$ into the quadratic kinetic term via a shift $Q_i \rightarrow Q_i - q_i$, where

$$q_i = \sum_j C_{ij} V_j - \frac{\sum_k V_k}{N} + \frac{Q}{N} \quad (7)$$

are the mean charges induced on the islands (we also include the i -independent contribution from the total charge Q for further convenience). This gauge transformation eliminates the $V_i Q_i$ terms in the Hamiltonian

(and adds a constant energy shift which we disregard). Under this transformation the wave functions pick up additional phases $\psi \sim \exp(i \sum_i q_i \phi_i)$; the new wave functions $\tilde{\psi}$ satisfy the twisted boundary conditions

$$\begin{aligned} \tilde{\psi}(\phi_1; \dots; \phi_{j+2}; \dots; \phi_N) \\ = \exp(i 2 \pi q_j) \tilde{\psi}(\phi_1; \dots; \phi_j; \dots; \phi_N) \end{aligned} \quad (8)$$

and the invariance under the continuous symmetry $\phi_i \rightarrow \phi_i + \alpha$ takes the form (c.f. (4)),

$$\tilde{\psi}(\phi_1 + \alpha; \dots; \phi_N + \alpha) = \tilde{\psi}(\phi_1; \dots; \phi_N); \quad (9)$$

We introduce the new variables $\phi_i = (\phi_1 + \dots + \phi_N)/N$ (conjugate to Q) and the gauge invariant phase drops over the junctions $\phi_i = \phi_{i+1} - \phi_i$, $a_{i,i+1}$ (out of N variables ϕ_i , only $N-1$ are independent, since $\sum_i \phi_i = 0$). The Hamiltonian then decouples into two, one involving only ϕ_i and the other only the phase drops ϕ_i . The continuous symmetry (9) implies that $\tilde{\psi}$ is independent of ϕ_i , i.e., $\tilde{\psi} = \tilde{\psi}(\phi_1; \dots; \phi_N)$. The boundary conditions on $\tilde{\psi}$ derived from (3) then take the form

$$\begin{aligned} \tilde{\psi}(\phi_1; \dots; \phi_{j+2}; \dots; \phi_{j+1} - 2\pi q_j; \dots; \phi_N) \\ = \exp(i 2 \pi q_j) \tilde{\psi}(\phi_1; \dots; \phi_j; \phi_{j+1}; \dots; \phi_N) \end{aligned} \quad (10)$$

and can be given a simple physical interpretation (see Fig. 2(a)): on moving a flux 2π (one flux quantum) around the j -th island the wave function gains a phase $2\pi q_j$.

We are now prepared for the calculation of the tunneling amplitude connecting the two semiclassical minima. Due to the equivalence of phase drops ϕ_i differing by a multiple of 2π , the coordinate space is a $(N-1)$ -dimensional torus. After unfolding the torus onto the plane, each point on the torus is represented by a lattice of points on the plane. We choose the point $\phi_i = 0$ as the representative of one of the two minima. The N neighboring minima with coordinates $\phi_i = 2\pi q_i / N$, $q_i = 1, \dots, N$ then correspond to the other minima. Accordingly, there are N different optimal tunneling trajectories connecting the two minima and we have to add up the various amplitudes coherently in order to find the hopping amplitude. Inspection of the particular phase changes along each of these trajectories shows that they may be thought of as describing a flux 2π entering the loop through the junction k and leaving the loop equally distributed (i.e., with a fraction $2\pi/N$ of flux per junction) among all the junctions, see Fig. 2(b). These trajectories exhibit different phase windings and thus are topologically different. The relative phases between these trajectories may then be read off the boundary conditions for the wave function $\tilde{\psi}$; e.g., the phase difference between the tunneling amplitudes for the trajectories k_1 and k_2 equals the phase difference of the wave function $\tilde{\psi}$ at the points $\phi_i = 2\pi q_i / N$; $q_i = 1, \dots, N$ and $q_i = 2\pi q_i / N$; $q_i = 1, \dots, N$.

and $\phi_i = 2\pi q_i / N$; $q_i = 1, \dots, N$. This phase difference is $2\pi (q_{k_1+1} + q_{k_1+2} + \dots + q_{k_2})$ and may be interpreted as the phase generated by the unit flux entering the loop through junction k_1 and leaving through junction k_2 (see Fig. 2(c)). From this argument immediately follows the result (1) for the level splitting (the level splitting in the double-well problem is proportional to the absolute value of the tunneling amplitude).

IV. LEVEL SPLITTING IN THE $E_J \ll E_C$ LIMIT

In the charge-dominated limit $E_J \ll E_C$ it is convenient to work in the charge representation¹³, where the operators Q_i are diagonal and the Josephson term in the Hamiltonian (2) takes the form (we restrict the discussion to tunneling junctions with $U_i(\phi) = E_J \cos(\phi)$)

$$H_J = \frac{E_J}{2} \sum_i L_i^+ L_{i+1} e^{i \phi_i} + \text{h.c.}; \quad (11)$$

with L_i^+ (L_i) the charge raising (lowering) operators on the i -th island, $L_i Q_i = Q_i L_i \pm 1$. The periodicity in Q allows us to restrict our analysis to the N charge sectors $Q = 0, \dots, N-1$. Below we first neglect the coupling E_J and find the ground states of the Coulomb part of the Hamiltonian; hopping between the islands is then perturbatively included in a second step.

We start with a diagonal matrix $(C^{-1})_{ij}$ and ignore the capacitive coupling of the junctions, i.e., the islands are coupled only to the ground but not to each other. In that case, the ground state of the Coulomb part of the Hamiltonian is C_N^Q -fold degenerate ($C_N^Q = N!/(N-Q)!$ enumerates the number of ways to distribute Q particles among N sites without double occupancy). Second, we solve the Hamiltonian (11) projected onto this C_N^Q -dimensional subspace in order to find the level splitting at finite E_J . This is easily done by observing the equivalence of this problem to the tight-binding model for hardcore bosons on the circle with N sites. Mapping to free

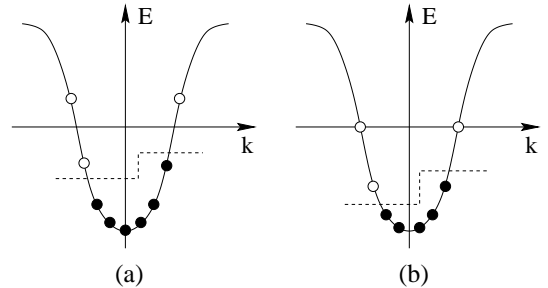


FIG. 3. The tight-binding spectrum on the circle with periodic (a) and anti-periodic (b) boundary conditions applying for even and odd Q , respectively. The solid circles denote filled states at the bottom of the band. For Q not divisible by N , the ground state is doubly degenerate. Q divisible by N corresponds to an empty (or filled) band.

fermions and taking into account the flux through the loop and the boundary conditions on the circle, one finds that the projected H_J describes a tight binding model for Q free fermions on a circle with N sites and periodic boundary conditions for even Q , while anti-periodic boundary conditions apply for odd Q (Fig. 3). This implies that the ground state is non-degenerate with a gap of order E_C if Q is divisible by N (the 'insulating state' with an empty band) and doubly degenerate (with the lowest excitation at an energy of the order of the intra-band level spacing E_J/N above the degenerate ground state) otherwise.

Turning on the junction capacitance makes the particles (Cooper pairs) repel each other and they tend to arrange in configurations with maximum separation between them. The number of such configurations is generally less (or equal) than C_N^Q . We conjecture that even in this case the ground state level is degenerate unless Q is divisible by N . We do not have a rigorous proof of this statement but have verified it for $N = 3, 4, 5$ (in fact, for $N = 3$ the off-diagonal elements of the matrix $(C^{-1})_{ij}$ may be incorporated in a constant term $\propto Q^2$ and do not change the properties of the system). The degeneracy may, of course, be explicitly verified for any given N and Q .

V. SYMMETRY ANALYSIS

In the previous sections, we have seen that the ground-state degeneracy depends on the divisibility of the total charge Q by the number of islands N and coincides in the two limits $E_J \ll E_C$ and $E_J \gg E_C$. In this section we show that this degeneracy is a consequence of the geometric symmetries of the loop and remains exact beyond the perturbation theory around these limiting cases. We shall classify the irreducible representations of the symmetry group of the loop, and identify the representations corresponding to the ground state. In both limits, the ground states correspond to the same representation, which implies that the degeneracy is also preserved in the intermediate parameter range, unless level-crossing occurs. We verify the absence of level-crossing in the

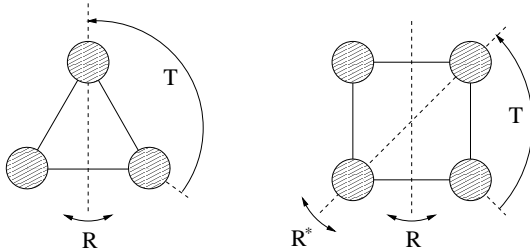


FIG. 4. Geometric symmetries of the Josephson junction loop for odd and even N involving translations T and reflections R . For even N , the two classes of reflections are related by $R = TR$.

several simplest cases numerically by exact diagonalization.

The level degeneracies for general values of $E_J = E_C$ are determined by the symmetry group of the Josephson-junction loop. The geometric symmetries are described by the dihedral group D_N consisting of cyclic permutations T of the islands (preserving the loop orientation; these are equivalent to a N -fold rotation axis) and of reflections R about diameters of the loop drawn through islands or through junctions, see Fig. 4. The reflections R reverse the flux through the loop and belong to its symmetry group for flux zero or half-quantum. The dihedral group D_N involves $2N$ symmetry operations; it may be characterized with the defining relations

$$T^N = 1; \quad (12)$$

$$R^2 = 1; \quad (13)$$

$$(TR)^2 = 1; \quad (14)$$

These relations are obeyed by the operators representing R and T at zero magnetic flux through the loop. On the other hand, for the case of half a flux quantum piercing the loop the symmetry operators preserving the Hamiltonian need to be supplemented by additional gauge transformations. As a consequence, the above relations are modified, with the appearance of additional phase shifts. Explicitly, the operators corresponding to rotations T and reflections R have the form

$$T (\phi_1; \dots; \phi_N) = (\phi_2; \dots; \phi_N; \phi_1); \quad (15)$$

$$R (\phi_1; \dots; \phi_N) = (\phi_N; \phi_{N-1} + 2\pi/N; \dots; \phi_1 + 2\pi(N-1)/N); \quad (16)$$

where the shifts $(2\pi/N)k$ of the phase ϕ_{N-k} compensate for the external vector potential in the Hamiltonian (2) and guarantee its invariance. This modifies the relation (13) producing an additional phase shift:

$$R^2 = \exp(-2iQ\pi/N); \quad (17)$$

The simplest way to make use of symmetry arguments is for the case N even and Q odd: we show that all states are degenerate in this case. Let us assume the opposite, i.e., that the eigenstate $|j\rangle$ is non-degenerate. Acting with T and R on $|j\rangle$ we reproduce the state up to phases t and r which satisfy the relations $t^N = (tr)^2 = 1$ and $r^2 = \exp(-2iQ\pi/N)$; this set of equations is inconsistent for N even and Q odd, hence all levels indeed are degenerate.

To determine the level degeneracy and to treat the case of arbitrary N and Q , we classify the representations of the symmetry group. To take into account the phase shift in (17), we include such phase shifts as new central elements $z = \prod_{j=1}^N z_j$ in the group. The resulting set of defining relations is

$$\begin{aligned} z^N = T^N = (TR)^2 = 1; \quad R^2 = z^{-1}; \\ zR = Rz; \quad zT = Tz \end{aligned} \quad (18)$$

TABLE I. Character table of the dihedral group D_N for N odd: the two one-dimensional representations are denoted by $D^{(\cdot)}$; the $(N-1)/2$ two-dimensional representations $D^{(\cdot)}$ involve the roots $t = \exp(2\pi i/N)$, with $t^N = 1$; $(N-1)/2 = 2$.

| | fEg | fT ; T | $g_{n=1}^{(N-1)/2=2}$ | fT ^m R $\prod_{m=0}^{N-1} g$ |
|------------------|-----|---------------------|-----------------------|---|
| D ^(·) | 1 | 1 | 1 | |
| D ^(·) | 2 | t + t ⁻¹ | | 0 |

TABLE II. Character table of ZD_N for N odd. The representations are classified by the charge Q which relates to the values of the central element $Z = \exp(2\pi iQ/N)$. The $2N$ one-dimensional representations are denoted by $D^{(\cdot; Q)}$; the $N(N-1)/2$ two-dimensional representations $D^{(\cdot; Q)}$ involve the roots $t = \exp(2\pi i/N)$. The indices n and m span the integers $n = 0; \dots; N-1$ and $m = 1; \dots; (N-1)/2$, respectively.

| | fZ^ng | fZ^nT | $;Z^{n+}T$ | $g^{(N-1)/2=2}_{n=1}$ | fZ^nT^{2m} | $R^{N-1}_{n=0}g$ |
|-----------------|---------|---------|----------------------|-----------------------|--------------|------------------|
| $D^{(\cdot;Q)}$ | Z^n | | $Z^{n+}=2$ | | | $Z^{n-1}=2$ |
| $D^{(\cdot;Q)}$ | $2Z^n$ | | $Z^{n+}=2(t+t^{-1})$ | | | 0 |

(the last two relations are equivalent to the statement that Z commutes with all group elements, i.e., it is a central element). The set of relations (18) defines a central extension of the group D_N which we further denote ZD_N . Extending D_N to ZD_N by the central element Z enlarges the number of elements in the group by a factor of N , and the number of elements of ZD_N is $2N^2$.

In any particular irreducible representation, Z is represented by a number (a N -fold root of unity, since $Z^N = 1$):

$$Z = \exp(2\pi iQ/N) \quad (19)$$

This formula establishes the relation between the representations of ZD_N and the total charge Q on the array.

Here we should mention that central extensions of symmetry groups are common in quantum mechanics. Indeed, the overall phase of the wave function has no physical meaning. Therefore the operator representing the product of two symmetry operations must equal the product of the two operators representing each of these operations only up to an overall phase factor. In other words, quantum mechanics admits not only linear representations of the symmetry group, but a more general class of projective representations⁹. At the same time any projective representation of a group corresponds to a linear representation of a central extension of this group. Physical examples are numerous, including half-integer spin (projectively representing the rotation group), magnetic translations (projectively representing geometric translations), and anyons (projectively representing the braid group). An example resembling the analysis in the present paper is given by Kalatsky and Pokrovsky¹⁴ in

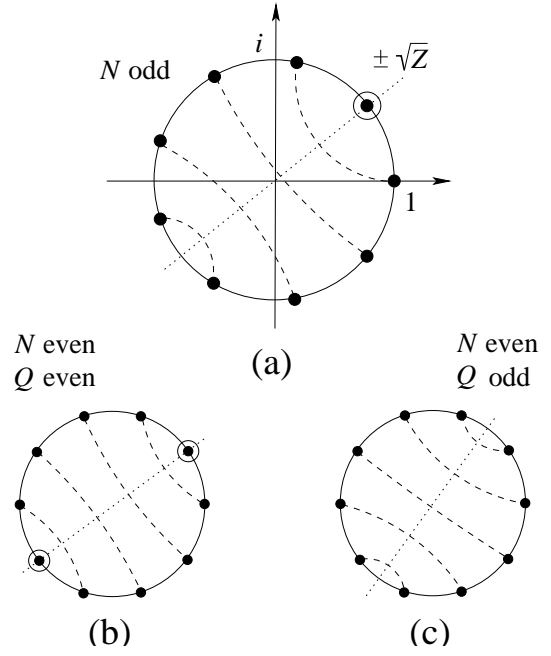


FIG. 5. The irreducible representations of ZD_N may be distinguished by the eigenvalues of the operator T . These eigenvalues must belong to the set of N -fold roots of unity $\{\exp(2\pi i m/N)\}$ (m marked by filled dots on the unit circle). The dotted line is drawn to intersect the unit circle at points $\pm\sqrt{Z}$. (a) N odd: exactly one of the square roots $\pm\sqrt{Z}$ is a N -fold root of unity. It gives the eigenvalue of T involved in the one-dimensional representations $D^{(\cdot; Q)}$ (marked by a small circle around the filled dot). The rest of allowed eigenvalues combine in pairs to form two-dimensional representations $D^{(\cdot; Q)}$ (the corresponding pairs of dots are connected by dashed lines). (b) and (c): the corresponding illustrations for even N and even Q , and for even N and odd Q respectively.

their discussion of the spectrum of large spins in external crystal electric fields; the degeneracies then are described in terms of projective representations of a finite symmetry group which depend on the spin assuming integer or half-integer values.

In the following we first review the irreducible representations of D_N and then discuss how it is modified when D_N is extended to ZD_N .

Consider first the case with an odd number of islands N . Using the defining relations (12)-(14) we arrange the $2N$ elements of the group D_N into the $(N+3)/2$ conjugacy classes: fEg, fT ; T $g_{n=1}^{(N-1)/2=2}$, and fT^m R $\prod_{m=0}^{N-1} g$. Firstly, we can construct two one-dimensional representations $D^{(\cdot)}$ where all operators are represented by numbers. In these representations, the value of T is determined uniquely: $D_T^{(\cdot)} = 1$, while R may take two values: $D_R^{(\cdot)} = \pm 1$. In addition, we can find $(N-1)/2 = 2$ representations $D^{(\cdot)}$ with dimensionality two. The explicit form of T and R in these representations is:

$$D_T^{(\cdot)} = \begin{pmatrix} t & 0 \\ 0 & t^{-1} \end{pmatrix}; \quad D_R^{(\cdot)} = \begin{pmatrix} 0 & 1 \\ 1 & 0 \end{pmatrix}; \quad (20)$$

TABLE III. Character table of the dihedral group D_N for N even: the four one-dimensional representations are denoted by $D^{(\cdot)}$; the $N=2$ two-dimensional representations $D^{(\cdot)}$ involve the roots $t = \exp(2i\pi/N)$ with $\cdot = 1; \dots; N=2-1$.

| | fEg | $fT; T g_{n=1}^{N=2-1}$ | $fT^{N=2}g$ | $fT^{2m}R_{\frac{N}{2}=0}^{N=2-1}g$ | $fT^{2m+1}R_{\frac{N}{2}=0}^{N=2-1}g$ |
|-----------------|-------|-------------------------|--------------|-------------------------------------|---------------------------------------|
| $D_+^{(\cdot)}$ | 1 | 1 | 1 | 1 | 1 |
| $D_-^{(\cdot)}$ | 1 | (-1) | $(-1)^{N=2}$ | 1 | 1 |
| $D^{(\cdot)}$ | 2 | $t + t$ | $2(-1)$ | 0 | 0 |

TABLE IV. Character table of ZD_N for N even. The representations are classified by the charge Q which relates to the values of the central element $Z = \exp(2iQ/N)$. The $2N$ one-dimensional representations $D^{(\cdot; Q)}$ exist for even Q ; the $N(N-1)=2$ two-dimensional representations denoted by $D^{(\cdot; Q)}$ involve the roots $t = \exp(2i\pi/N)$. The indices n, m , and \cdot span the integers $n = 0; \dots; N-1$, $m = 0; \dots; N=2-1$, and $\cdot = 1; \dots; N=2-1$, respectively; the index \cdot runs over the half-integers $\cdot = 1/2; 3/2; \dots; (N-1)/2$.

| | $fZ^n g$ | $fZ^n T; Z^{n+1} T g_{n=1}^{N=2-1}$ | $fZ^m T^{N=2}; Z^{m+N=2} T^{N=2} g$ | $fZ^m T^{2n} R_{\frac{N}{2}=0}^{N=2-1} g$ | $fZ^m T^{2n+1} R_{\frac{N}{2}=0}^{N=2-1} g$ |
|---------------------------------|----------|-------------------------------------|-------------------------------------|---|---|
| $D_+^{(\cdot; \text{even } Q)}$ | Z^n | $Z^{n+1/2}$ | $Z^{m+N=4}$ | $Z^{m-1/2}$ | Z^m |
| $D_-^{(\cdot; \text{even } Q)}$ | Z^n | $(-1) Z^{n+1/2}$ | $(-1)^{N=2} Z^{m+N=4}$ | $Z^{m-1/2}$ | Z^m |
| $D^{(\cdot; \text{even } Q)}$ | $2Z^n$ | $Z^{n+1/2} (t + t)$ | $2(-1) Z^{m+N=4}$ | 0 | 0 |
| $D^{(\cdot; \text{odd } Q)}$ | $2Z^n$ | $Z^{n+1/2} (t + t)$ | 0 | 0 | 0 |

where the parameter labeling representations takes integer values $1; \dots; (N-1)/2$, and $t = \exp(2i\pi/N)$. We thus have found all the $(N+3)/2$ irreducible representations; they are listed in the character TABLE I.

The irreducible representations of the extended dihedral group ZD_N are found in an analogous way. Assume N odd first. Then ZD_N contains $N(N+3)/2$ conjugacy classes: $fZ^n g_{n=0}^{N-1}$, $fZ^n T; Z^{n+1} T g_{n=0}^{(N-1)/2}$, and $fZ^m T^{2m} R_{\frac{N}{2}=0}^{N=2-1} g$. The construction of the irreducible representations again follows the scheme described above: for one-dimensional representations $D^{(\cdot; Q)}$ we find $2N$ solutions: $D_T^{(\cdot; Q)} = \frac{1}{\sqrt{2}} Z$ and $D_R^{(\cdot; Q)} = \frac{1}{\sqrt{2}} \bar{Z}$, where we choose that branch of the square root which puts $\frac{1}{\sqrt{2}} Z$ onto one of the roots $\exp(2i\pi/N)$ [for odd N either $\frac{1}{\sqrt{2}} Z$ or $\frac{1}{\sqrt{2}} \bar{Z}$ belongs to the set $\{ \exp(2i\pi/N) \}_{n=0}^{N-1} g$, see Fig. 5]. The remaining two-dimensional representations $D^{(\cdot; Q)}$ may again be constructed explicitly:

$$D_T^{(\cdot; Q)} = \frac{1}{\sqrt{2}} \begin{pmatrix} t & 0 \\ 0 & t^{-1} \end{pmatrix}; \quad D_R^{(\cdot; Q)} = \frac{1}{\sqrt{2}} \begin{pmatrix} 0 & 1 \\ 1 & 0 \end{pmatrix}; \quad (21)$$

where for $\frac{1}{\sqrt{2}} Z$ we again take one of the roots $\exp(2i\pi/N)$, the parameter takes integer values $1; \dots; (N-1)/2$, and $t = \exp(2i\pi/N)$. With $2N$ one-dimensional and $N(N-1)/2$ two-dimensional representations we then have constructed all irreducible representations of ZD_N . The result is summarized in TABLE II.

A similar analysis for the qubit loop with an even number N of junctions produces the character TABLES III and IV for the groups D_N and ZD_N respectively.

In summary, the energy levels of the Josephson junction loop may be classified according to the irreducible

representations of its symmetry group ZD_N at a given Q . The representation tables (Tables II and IV) look slightly different for odd and even N . All representations are either one- or two-dimensional. Given an odd N , for any value of Q , there are two one-dimensional representations and $(N-1)/2$ two-dimensional representations. Given an even N , for even Q we have four one-dimensional and $(N=2-1)$ two-dimensional representations, while for odd Q there are no one-dimensional and $N=2$ two-dimensional representations. The representations may be distinguished by the eigenvalues of the operator T involved, see Fig. 5.

Connecting back to our physical problem we can find the degeneracy of the states: for example, when N is even and Q is odd (see Fig. 5(c)) all states (including the ground state) are doubly degenerate. More work is needed to determine whether the ground state is degenerate in the other cases. Inspection of the ground state wave functions in the limits $E_J \ll E_C$ and $E_J \gg E_C$ shows that they transform with a representation involving the eigenvalues $T = 1$ and $T = \exp(2iQ/N)$. Indeed, in the $E_J \ll E_C$ limit, the state $f_i = -Ng$ is a $T = 1$ eigenstate, while the state represented by the points $f_i = -Ng; i \notin k; k = -N/2, \dots, N/2-1$ by virtue of (10) belongs to the eigenvalue $T = \exp(2iQ/N)$. In the limit $E_J \gg E_C$, T measures the total momentum of the repulsive bosons which (for a diagonal capacitance matrix) equals the total momentum of the tight-binding fermions. The latter is easily read off Fig. 3 and accounting for the shift Q/N due to the boundary condition (originating from the half-quantum flux) we again obtain the two eigenvalues $T = 1$ and $T = \exp(2iQ/N)$ for the two lowest states. Thus if $Q \notin 0 \pmod{N}$ the two lowest states combine into a

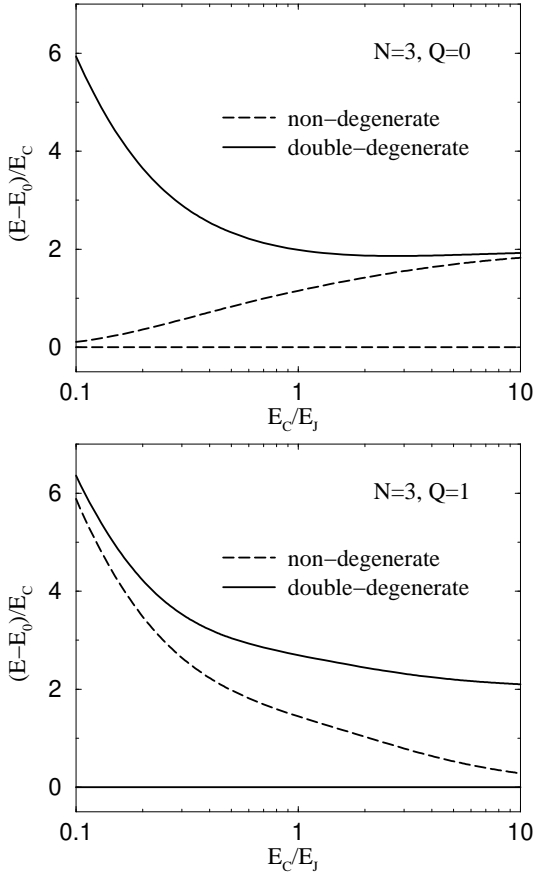


FIG. 6. The two lowest excitation energies for the symmetric Josephson junction loop with $N = 3$ islands, diagonal capacitance matrix $(C^{-1})_{ij} = E_{Cij}$, and vanishing gate voltages $V_i = 0$. The ground-state energy at each value of $E_C = E_J$ is subtracted. (a) in the $Q = 0$ sector where the ground state is non-degenerate; (b) in the $Q = 1$ sector with the ground state doubly degenerate. Note the large (small) gap of order E_C ($E_J = N$) for the insulating state with $Q = 0$ (the metallic state with $Q = 1$) in the limit $E_C = E_J \rightarrow 1$.

two-dimensional representation (and the same in both limits), resulting in a doubly degenerate ground state. For Q divisible by N , the ground state corresponds to a one-dimensional representation of ZD_N , i.e., it is non-degenerate. As the ratio $E_J = E_C$ is swept from one limit to the other, the ground state continuously evolves preserving its degeneracy, unless a level-crossing occurs with a level of different symmetry. We have numerically that such a level crossing does not occur for the cases $N = 3$ and $N = 4$ using a diagonal capacitance matrix $(C^{-1})_{ij}$, (the results for $N = 3$ are shown in Fig. 6), and we believe that this property holds for any $N \geq 3$.

The experimental observation of the quantum interference effect discussed in this paper relies on several requirements on the Josephson junction loop. First, we have to assume that all quasiparticles are frozen out, which defines an upper bound on the temperature roughly estimated as $T < T_{sc} = \log(\rho_0 V_{sc})$, where ρ_0 is the density of states at the Fermi level, V_{sc} is the superconducting gap, and V is the volume of the system¹⁵. For a micrometer-size aluminum loop similar to that used in the experimental work of van der Wal et al.¹¹, $T_{sc} = 1.5 - 100$ mK and can be easily achieved.

Second, we assume that no charge tunneling is possible onto the array. In practice, we may allow the array to be connected to an external reservoir via a large resistor (to be able to change the charge on the array by an overall shift of gate voltages). Its resistance then must be much larger than the characteristic resistance scale $R = (C)^{-1}$, where C is the capacitance of the array, and \hbar is the relevant energy scale (of the order of the splitting between the two lowest states). In the charge-dominated limit, E_C and R is of the order of the resistance quantum $\hbar/4e^2$, in agreement with the conventional condition for charge quantization in the Coulomb blockade setup¹⁶. In the phase-dominated limit, E_C and R is much larger than the resistance quantum. Also, under the condition $\hbar_{sc} > E_C^{\text{loop}}$ a 'weak' contact to the external world would allow an unpaired quasiparticle to escape from the loop, leaving only paired electrons in the system.

Third, the islands and the junctions are assumed to be identical. The precision to which this symmetry has to hold in the phase-dominated limit may be simply estimated from the condition that the tunneling actions agree up to small deviations of order one. The tunneling action scales as $S = (E_J = E_C)^{1/2}$ and therefore the required precision is $(E_J = E_C) / (E_C = E_C) \sim S^{-1}$. For a detectable splitting S must be not too large; for a qubit design, S is typically^{6,8} taken to be of order 5-10, and these conditions may well be satisfied.

The required precision on the magnitude of the external magnetic field (or, equivalently, on the flux through the loop) may be estimated from the condition that the level splitting due to the deviation of the flux from $\phi_0 = 2$ is much smaller than that from the tunneling between the qubit states. In the phase-dominated limit ($E_J \gg E_C$) this produces the condition $E_J = \phi_0$ and hence $\phi = \phi_0 \pm S^{-1}e^S$. In the opposite charge-dominated limit, it is sufficient to require that $\phi = \phi_0 \pm 1$.

In conclusion we have discussed the spectral properties of symmetric Josephson junction loops, devices similar to those recently proposed as potential qubits for quantum computing^{6,8}. While in the charge-dominated regime with $E_C \gg E_J$ the dependence of the ground-state degeneracy on the total charge on the island is a

simple charging effect, this degeneracy derives from a subtle quantum interference in the phase-dominated limit $E_J \gg E_C$. Several proposals on solid state realizations of quantum bits belong to the latter limit. From our analysis it follows that the requirements for observing the charge dependence of the qubit-level splitting are similar to those for the qubit operation (plus symmetry requirements which are easy to satisfy). The interference effects studied in this paper then may serve as a good test of quantum coherence in such qubit designs.

We thank M. Feigelman and O. Hallatschek for helpful discussions, and M. Troyer for providing the exact diagonalization code. We thank the Swiss National Fonds for financial support. L. I. thanks ETH Zurich for hospitality.

-
- ¹ R. S. Newrock, C. J. Lobb, U. G. Eichenmüller, and M. Octavio, "The two-dimensional physics of Josephson junction arrays", *Solid State Physics* 54 (2000), 263, and references therein.
 - ² Ya. M. Blanter, R. Fazio, and G. Schon, "Duality in Josephson junction arrays", *cond-mat/9701223* and in *Nucl. Phys. B*.
 - ³ Y. Aharonov and A. Casher, "Topological quantum effects for neutral particles", *Phys. Rev. Lett.* 53 (1984), 319.
 - ⁴ W. J. Elion, J. J. W. Achters, L. L. Sohn, and J. E. Mooij, "Observation of the Aharonov-Casher effect for vortices in Josephson-junction arrays", *Phys. Rev. Lett.* 71 (1993), 2311.
 - ⁵ A. Shnirman, G. Schon, and Z. Hermon, "Quantum manipulations of small Josephson junctions", *Phys. Rev. Lett.* 79 (1997), 2371.
 - ⁶ T. P. Orlando, J. E. Mooij, L. Tian, C. H. van der Wal, L. S. Levitov, S. Lloyd, and J. J. M. Aza, "Superconducting persistent-current qubit", *Phys. Rev. B* 60 (1999), 15398.
 - ⁷ L. B. Ioé, V. B. Geshkenbein, M. V. Feigelman, A. L. Fauchère, and G. B. Lattar, "Environmentally decoupled sds-wave Josephson junctions for quantum computing", *Nature* 398 (1999), 679.
 - ⁸ G. B. Lattar, V. B. Geshkenbein, and L. B. Ioé, "Engineering superconducting phase qubits", e-print *cond-mat/9912163*.
 - ⁹ See e.g. A. O. Barut and R. Raszka, "Theory of group representations and applications", *World Scientific*, Singapore 1986.
 - ¹⁰ C. H. van der Wal and J. E. Mooij, "Controlled single-Cooper-pair charging effects in a small Josephson junction array", *J. Superconduct.* 12 (1999), 807.
 - ¹¹ C. H. van der Wal, A. C. J. ter Haar, F. K. Wilhelm, R. N. Schouten, C. J. P. M. Hamans, T. P. Orlando, S. Lloyd, and J. E. Mooij, "Quantum superposition of macroscopic persistent-current states", *Science* 290 (2000), 773.
 - ¹² D. A. Ivanov and M. V. Feigelman, "Coulomb effects in a ballistic one-channel S-S device", *Zh. Eksp. Teor. Fiz.* 114 (1998), 640 [*J. Exp. Theor. Phys.* 87 (1998), 349; e-print

cond-mat/9712074].

- ¹³ P. Lafarge, M. M. Atters, and J. E. Mooij, "Charge representation of a small two-dimensional Josephson-junction array in the quantum regime", *Phys. Rev. B* 54 (1996), 7380.
- ¹⁴ V. A. K. alatsky and V. L. Pokrovsky, "Spectra and magnetic properties of large spins in external fields", *Phys. Rev. A* 60 (1999), 1824.
- ¹⁵ M. T. Tuominen, J. M. Hergenrother, T. S. Tighe, and M. Tinkham, "Experimental evidence for parity-based 2e periodicity in a superconducting single-electron tunneling transistor", *Phys. Rev. Lett.* 69 (1992), 1997.
- ¹⁶ D. V. Averin and K. K. Likharev, in *Mesoscopic Phenomena in Solids*, edited by B. Altshuler et al. (Elsevier, Amsterdam, 1991).